Design of MEMS vision tracking system based on a micro fiducial marker

Yong-Sik Kim [a], Seung Ho Yang [b,*], Kwang Woong Yang [c], Nicholas G. Dagalakis [a]

[a] Intelligent System Division, Engineering Laboratory, National Institute of Standards and Technology, 100 Bureau Dr. Gaithersburg, MD 20,899, USA
[b] HDI Tech. Staging, Shakopee Drive Center, Seagate Technology, Mailstop SHK221, 1280 Disc Drive, Shakopee, MN 55379, USA
[c] Korea Institute of Industrial Technology, Cheonan, South Korea

ARTICLE INFO

ABSTRACT

Many microelectromechanical systems (MEMS) devices require considerable design effort to embed their own sensors to monitor themselves.

In this study, a MEMS-based vision tracking system is developed based on micro fiducial markers. The vision tracking system recognizes the predetermined patterns of the micro-scale fiducial markers and calculates the position and rotation of the MEMS elements. Due to its good accessibility, the presented system can be applied to MEMS devices without significant effort or modification. This tracking system and three micro vision markers are applied to a MEMS nanopositioner as a linear displacement sensor. With three fiducial markers printed on a nanopositioner, the presented system can monitor the linear displacement of the nanopositioner with the error less than 1% of an intended motion and the jitter error less than 1 μm. The presented MEMS vision tracking system also demonstrated its capabilities to track multiple MEMS elements simultaneously in MEMS-based micro-manipulation.

1. Introduction

The small footprint, nanometer level resolution and low cost of microelectromechanical systems (MEMS) extended the capabilities of the traditional motion stages to newer areas, including scanning probe for data storage scanning [1] and micro-manipulation inside a vacuum chamber [2]. Due the small form factor of MEMS elements, the macroscopic sensing techniques are of limited applicability. Therefore, how to sense and control the moving MEMS elements has been an issue. In order to solve this issue, many researchers attempted to develop motion sensing mechanisms which have similar or smaller form factor to combine them with the moving MEMS elements [3–16]. These efforts have led to the development of capacitive sensors, piezoelectric sensors, and optical sensors based on MEMS technologies that are widely used.

Capacitive sensors have been commonly used as linear displacement sensors [3,4], accelerometers [5], and a force sensor [6]. Capacitive sensors convert the gap change between two electrodes into a change in capacitance providing nanometer level resolution and intuitive design. Although popular in MEMS, capacitive sensors are vulnerable to other electrical noise and tend to occupy large area for better accuracy [7]. Therefore, in order to have meaningful results, considerable areas are required to monitor multiple objects or two or more degrees-of-freedom (DOF) motions.

Another popular sensor in MEMS is a piezoresistive sensor. Piezoresistive sensors are based on the resistance change of silicon under a stress [8]. Compared to a geometric change, the piezoresistive property of silicon has a large change in its resistance. The advantages of piezoresistive sensors are its relatively small size than capacitive sensors, high bandwidth, and nanometer level resolution [9]. But, in order to implement this sensor, selective ion implantation or diffusion doping is required, and that may change the whole fabrication process of MEMS elements [10]. Thermal drift or flickering noise from piezoresistive sensors also require additional post-processing to eliminate them [8,10].

Contrary to capacitive and piezoresistive sensors, optical sensors can minimize additional design effort to embed the sensor on MEMS elements, because the monolithic design of MEMS provides reasonable field of view to an optical microscope installed on top of it. In addition to this advantage, optical sensors are immune against any noise related to electric or magnetic fields [11]. Intensity-based optical sensor measures the intensity of the light reflected on the surface of MEMS devices [12]. When MEMS devices move away from the irradiated light, the intensity of the reflected light will decrease. This can be measured quantitatively to extract the displacement information [13]. But, the intensity based sensors are

sensitive to ambient light intensity and vulnerable to its neighboring noise, therefore interferometric algorithms should be added to eliminate optical noise and improve its sensing performance [14–16].

Taking these backgrounds into consideration, it is rare to find MEMS-based sensors to monitor multiple objects at a same time without a lot of design efforts. Thus it is beneficial to develop a position sensor to monitor multiple MEMS elements simultaneously and also provide the similar performance to previous MEMS-based sensors without considerable design modification. Among the various sensing principles, a vision tracking system with micro fiducial markers can monitor multiple objects simultaneously and also provides reasonable performance [11,17]. A fiducial marker is a predetermined pattern mounted in the environment or on a target and is designed to be automatically detected by a vision tracking system based on an accompanying detection algorithm. They have been widely used in Augmented Reality (AR) [18], robot navigation [19], indoor localization [20]. In most cases, a fiducial marker is a 2D planar pattern, thus this can be transferred onto monolithic MEMS structures without significant effort. A charge-coupled device (CCD) camera is attached to an optical microscope to detect micro-scale fiducial markers and to get their images. Once the image of a fiducial marker is obtained, 3D positional information of a MEMS object can be monitored in real time with its own ID number.

In this study, a vision based tracking system is developed to monitor the position of MEMS elements based on micro fiducial markers. This vision tracking system is implemented with Microsoft Visual C++[1] 10.0 complier and an open computer vision library OpenCV[1] [21,22]. A PointGrey[1] Scorpion camera with its FlyCapture[1] software is utilized to access images. In order to demonstrate its capabilities, the present vision tracking system monitored the positions of three to five MEMS elements in real time. In addition to this, this vision tracking system is adopted as a linear displacement sensor for a MEMS-based nanopositioner where two micro fiducial markers are placed on the nanopositioner and one fiducial marker is on a fixed ground surrounding the nanopositioner. The relative position information among them can calibrate current optical set-up and also calculate the displacement of the movable part of the MEMS nanopositioner.

2. Design of the micro fiducial marker

The micro fiducial marker is introduced to provide information on translational and rotational information of MEMS elements in real time. It is a square border of white on black or black on white pattern and its interior is divided by a 4 × 4 square grid as shown in Fig. 1 [19]. The whole micro fiducial marker is 6 × 6 units including its border and has 16 cells to deliver its information. Each cell carries one bit of digital data with black or white color, so the information of 2^{16} can be stored in the micro fiducial marker. The cell at the corner A in Fig. 1 has the same color as its exterior border and the three cells at corner B, C, and D have different color from its border. This relationship determines the origin of the micro fiducial marker. In this case, we set up a rule that the origin will be the adjacent corner nearest to the cell at the corner A. The two edges adjacent to the origin will be assigned as an X-axis and a Y-axis and a Z-axis will be determined based on right-handed Cartesian Coordinates as shown in Fig. 1. The following position information will be expressed based on this origin.
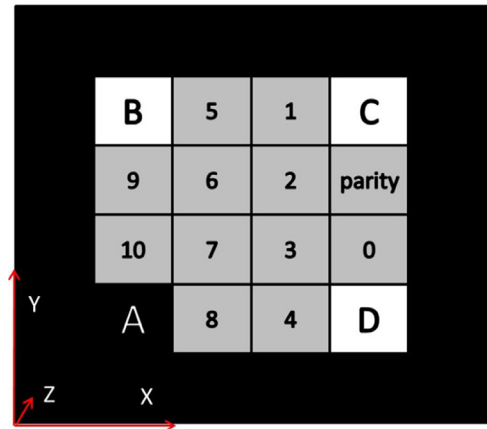
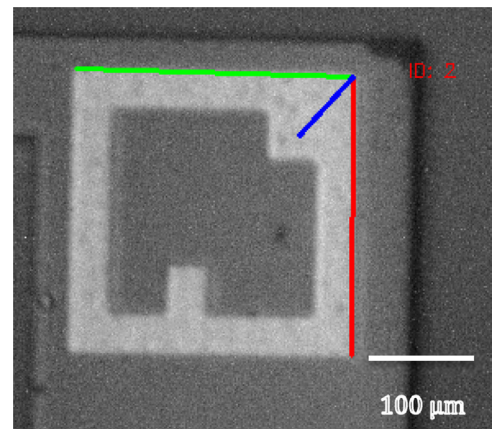**Fig. 1.** The conceptual design of the micro fiducial marker.

Fig. 2. The recognized micro fiducial marker.

Once the origin was determined, the information will be extracted from the interior cells, especially identity information to differentiate one from multiple micro fiducial markers. Twelve cells except the four at the corners are utilized to contain its ID. Based on its position relative to the origin, each cell was designated to its own number as shown in Fig. 1. When a cell has the same color as the wall, it will be counted to calculate its ID. When the total number of n is counted, its ID will be calculated based on Eq. (1).

$$\text{ID} = 2^a + 2^b + 2^c + \cdots + 2^n \tag{1}$$

where, superscript represents the number shown in Fig. 1 corresponding to the cell included in this calculation. For example, if the blocks with numbers 2 and 4 have the same color with the wall, the ID of this marker will be $2^2 + 2^4 = 20$. With this method, a total of 2^{11} or 2048 distinct IDs are available. In addition to this, one block close to C, shown in Fig. 1, is reserved for checking parity to avoid any incorrect recognition.

Fig. 2 is the capture of a micro fiducial marker once it is recognized by the vision tracking system. This marker has two blocks of a same color with its wall. In this case, the upper right corner will be designated as an origin and its ID will be 2 according to Fig. 1. Once it is recognized as a fiducial marker, its corresponding coordinate will display on the origin of the fiducial marker, where the green bar represents the X-axis, the red is the Y-axis, and the blue is the Z-axis.

This micro fiducial marker can be implemented by MEMS fabrication methods which can transfer a micro fiducial marker image onto a surface of MEMS elements. In this study, the fiducial markers are located at predetermined locations on the MEMS surfaces
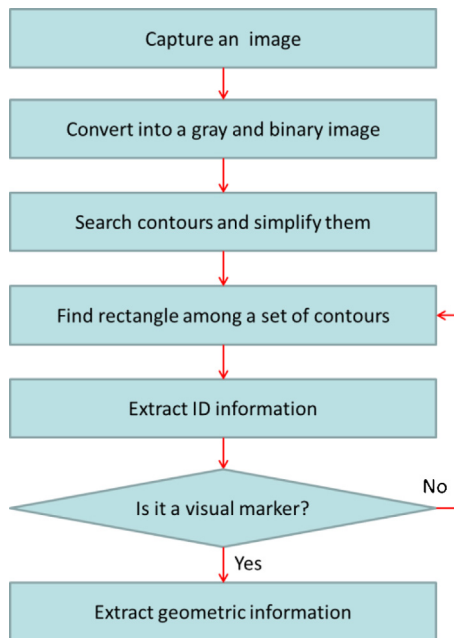
Fig. 3. Image processing procedure.

Fig. 5. Extraction of ID information: (a) a raw micro fiducial markers, (b) a recognized 6 × 6 grid information based on (a).

3.1. Pre-process of a captured image

The pre-processing filters out useless portions of image data and selects only the useful portions in a captured raw image for fast processing and better detection. For this, a captured image is converted into a grey one to reduce its total image size for quick processing with cvCvtColor function in OpenCV. Then, the converted grey image is filtered out again to eliminate noises with cvSmooth function in OpenCV. This image is then converted into a binary image with cvAdaptiveThreshold function in OpenCV. The adaptive threshold method converts a law image into a binary one by determining a threshold value based on its neighboring pixels. After this process, the candidates for micro fiducial markers become clearer, which is shown in Fig. 4(a) and Fig. 4(b). The fiducial markers made of gold are brighter than silicon itself, so the binary image has white fiducial markers and black background. Here, both gold and silicon are shiny, so the starting threshold value for a binary conversion was determined after multiple manual tests Fig. 5.

Most MEMS elements are very clean and well protected from dust and also hard to have any metal structures similar to the micro fiducial markers. Therefore a converted binary image tends to be clearer than normal environment and detected well by the presented vision tracking system without serious problems.

3.2. Search candidates for micro fiducial markers

After the pre-processing, the converted image is ready to find fiducial markers. The vision tracking system start looking for contours as candidates with the cvFindContours function in OpenCV. Once contours are found from the converted binary image, they will be simplified to a piece of lines if some points in a contour are on a same line. After all candidates are found and simplified, a contour having more than four points is selected as candidates from the fact that a fiducial marker is in a rectangular shape. If a selected contour

by depositing a thin metal layer made of chromium of 100 nm thick and gold of 200 nm thick with a lift-off process [23]. Since gold can be clearly detected on the surface of silicon, this metal pattern can be utilized as a fiducial marker. This can be replaced by any etching process if the process can change the surface color partially to transfer a fiducial marker image.

3. Design of the vision tracking system

The vision tracking system is designed to process and analyze captured image to extract meaningful information. The image processing procedure is described in Fig. 3, where the process consists of pre-processing, extracting candidates, finding fiducial markers, verifying fiducial markers, and calculating position information. A series of the recognition process for fiducial markers was implemented in a C++ programming environment (Visual Studio 10[1]) based on the image processing libraries (OpenCV[1]). The communication with a CCD camera is implemented with application programming interface (API) provided by PointGrey[1] camera.
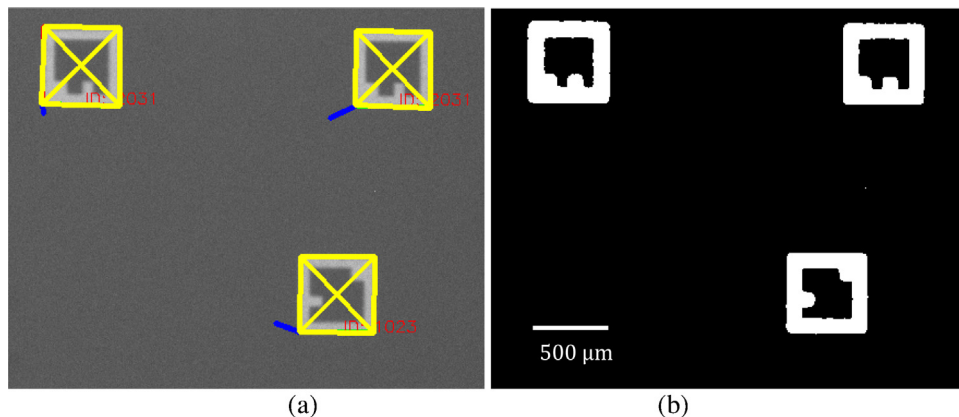

Fig. 4. Pre-processing of a captured image: (a) an original raw image with recognized fiducial markers, (b) a converted binary image of (a).
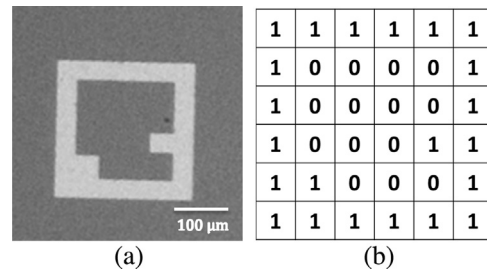
has a possibility to be a rectangle, its area will be compared with an imaginary rectangle fitting well with that contour. If this difference is acceptable or small enough and the middle point among four points of the imaginary rectangle is in the middle of the contour, this contour will be regarded as a fiducial marker candidate and be handed over the following process to extract its ID and 3D position information.

3.3. Extract ID information and position information from the candidates

The contour set selected in a previous section will be inspected to extract its ID number and position information. Frist, the four corners of a candidate will be recalculated to get more accurate results with cvFindCornerSubPix function in OpenCV. The image of the candidate then will be copied and mapped onto a square, which is divided by 6×6 grids. Inorder to have accurate results, each grid has 2×2 pixels for its data. This means the fiducial marker should be larger than 12×12 pixels from captured images. After this mapping process, an average pixel value of all grids is calculated and a maximum value will be set as 1 and a minimum value will be set as 0. All the remaining values will be normalized between these maximum and minimum values. If the normalized value of a grid is higher than an average value, that grid will be given a value of 0. If not, it will be given a value of 1. This value comes from the fact that golden patterns are brighter than silicon in MEMS. After the values for the entire grids are determined, these 6×6 grids are used to calculate its ID information based on Eq. (1) and Fig. 1. With this, a micro fiducial marker will be verified again by checking its parity which will keep the total number of 1 in the 6×6 grids even.

After a series of detection and verification, the 3-dimensional position information can be extracted by transforming the four corners of a micro fiducial marker in 3D space onto those on 2D captured image. For this, it is necessary to get the intrinsic matrix and distortion coefficients of a camera with the cvFindExtrinsicCameraParams2 function in OpenCV. This matrix and the coefficients are obtained through the calibration process of a camera used to capture fiducial markers.

3.4. Calibration of a camera

In order to calculate accurate 3D position information, it is necessary to calibrate the camera attached to an optical microscope precisely. Since most cameras create their own minor distortions to images, it is necessary to calibrate a camera first to achieve accuracy. In this study, the camera calibration is done using Zhang's flexible camera calibration method [24] which is utilized with a checker board pattern. The checker board pattern in this calibration is in micro-scale and fabricated with MEMS fabrication methods. When 24 positions in the checker board are well recognized, imaginary lines are displayed as shown in Fig. 6 and that area is calibrated. This process was repeated several times at different positions to calibrate a full field of view of the camera.

4. Application: a linear displacement sensor for a MEMS-based nanopositioner

4.1. Installation of three micro fiducial markers onto a MEMS-based nanopositioner

In order to demonstrate the usability of the presented vision tracking system, the presented system is installed on a MEMS-based nanopositioner as a linear displacement sensor. For this, a MEMS based 1-degree of freedom (DOF) nanopositioner shown in Fig. 7(a) is utilized, which is composed of a bent-beam type electrothermal actuator, two mechanical levers, two mechanical links,
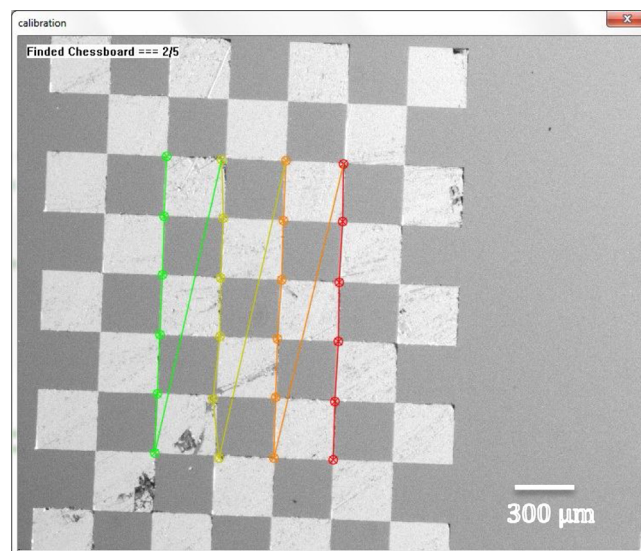

Fig. 6. The MEMS-based checker board recognized for the calibration of the camera connected to an optical microscope.

and a moving platform. When the electric current flows into the electrothermal actuator, the beams in the actuator will be expanded due to resistive heating. This expansion is converted into a linear displacement or a force along the central shaft and actuates the moving platform [2,12].

Four groups of fiducial markers are deposited on the surface of the nanopositioner as shown in Fig. 7(a). Each group is composed of three fiducial markers, whose close-up view is in Fig. 7(b), where the fiducial markers A, B, and C are located with their own ID numbers. The fiducial markers B and C are placed on a stationary boundary and the distance between them is 244.29 μm. This value is used as reference to calibrate the dimensions measured by the presented vision tracking system with different magnification ratios. The fiducial marker A is deposited on a movable component or a moving platform of the nanopositioner, so the displacement of the nanopositioner can be calculated by measuring the relative distance between the fiducial markers A and B and calibrating based on the fiducial markers B and C. Here, the three fiducial markers should be in a sight for its calibration and measurement. Since the distance between the fiducial markers B and C is 244.29 μm, the vision-tracking system can measure at least 244 μm with its current fiducial marker positions.

The fabrication of the nanopositioner shown in Fig. 7(a) with the fiducial markers in Fig. 7(b) follows standards Silicon-On-Insulator Multi-User Multi-Process (SOI-MUMPs) [25]. This process is composed of a metallization, with top side etching by Bosch process [26], and bottom side etching by same Bosch process. The first metallization process is to deposit metal pads for the electric connection of the nanopositioner, which is also utilized to transfer the fiducial markers on the surface of the nanopositioner.

4.2. Measurement of the displacement of the nanopositioner by the presented vision-tracking system

The nanopositioner is connected to a direct current (DC) power supply (Agilent[1] 3322A) generating a triangular or a rectangular waveform outputs with the amplitude of 5 V DC and a frequency of 0.1 Hz. The motions of the nano-positioner are measured by the presented vision-tracking system and their results are plotted in Fig. 8(a) with a triangular input and Fig. 8(b) with a rectangular one, respectively. Fig. 8(a) matches well with the fact that the displacement of the nanopositioner is proportional to the square of driving
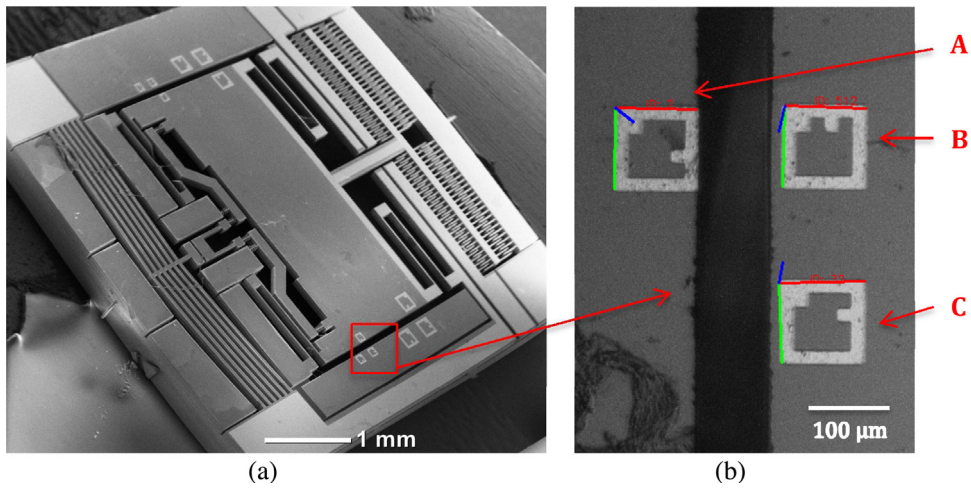
(a)   (b)

Fig. 7. The experimental set-up for the accuracy test: (a) a nanopositioner with four sets of the fiducial markers, (b) a close-up view of the recognized fiducial markers.
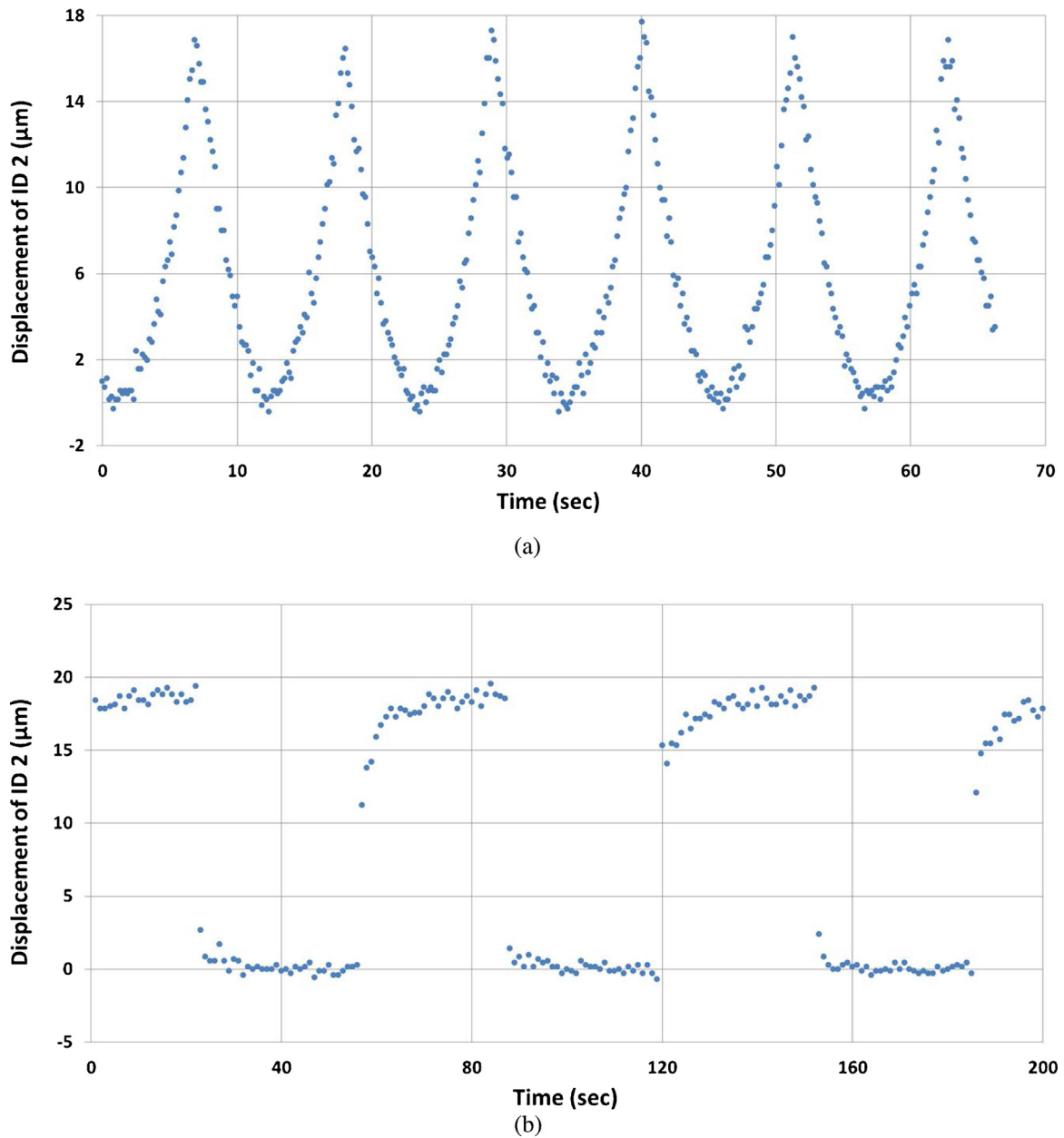

(a)

(b)

Fig. 8. The displacements of a MEMS nano-positioner platform measured by the vision-tracking system; (a) a triangular waveform input, (b) a square waveform input.
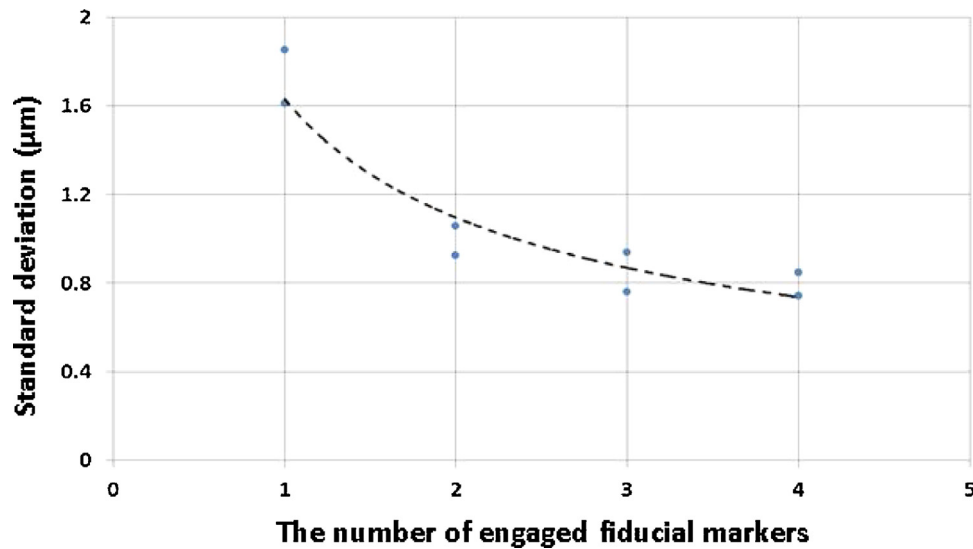
Fig. 9. A stability test with multiple fiducial markers.

voltage [2]. This is because the displacement of the nanopositioner is theoretically proportional to the current density, which is proportional to the square of the driving voltage. Fig. 8(b) shows a square motion with a distorted corner. This is because the electrothermal actuator used in the nanopositioner takes tens of milli-seconds to heat up and cool down the beams in the actuator.

Here, the displacement of the nanopositioner was measured four times by the vision-tracking system and turns out that motion is 17.861 μm after self-calibration. In order to evaluate its accuracy, the same motion is also measured multiple times by an external optical profiler (VEECO[1] NT1100 [27]). The displacement measured by this profiler is 17.731 μm. This comparison demonstrates that the presented vision tracking system is capable of measuring the distance with an error less than 150 nm or 1%. The average processing time from capturing one image to measuring its displacement varies from 40.7 ms to 148.8 ms depending on the number of the fiducial markers to monitor. This indicates that the presented vision tracking system can provide 6.7–24 measurements per a second. A microscope with a lower magnification ratio can increase its maximum range to measure, but it decreases its accuracy due to poor image quality or lower resolution.

4.3. Reliability and stability of the vision-tracking system

The stability of the vision-tracking system is also numerically estimated by monitoring the position of stationary fiducial markers or a jitter test. The same nano-positioner with multiple fiducial markers is utilized for this test and its result is plotted in Fig. 9, where one to four fiducial markers are engaged for this test. With a single fiducial marker, the presented system has a standard deviation of about 1.6–1.8 μm for 115 s. When two fiducial markers are used for this test, the standard deviation decreases to 1–0.9 μm. This standard deviation tends to converge around 0.8 μm with three or more fiducial markers. Based on this observation, the presented vision tracking system can provide a stability error of approximately 1 μm for 115 s with two fiducial markers, because it is not practical to involve more than two fiducial markers on a small MEMS device.
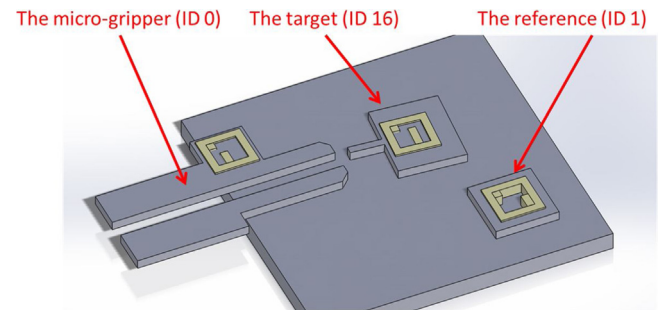

Fig. 10. The basic elements for the micro-manipulator with three fiducial markers.

5. Application: monitoring a multiple elements in micro-manipulation

5.1. The micro-manipulation system layout

Another relevant application with the presented vision tracking system is a micro-manipulation, which requires monitoring multiple objects at the same time. The basic elements for the micro-manipulation system are shown in Fig. 10, which shows the micro-gripper (ID 0), the micro-scale object to move (ID 16), and the reference (ID 1). The three components have their own fiducial markers with unique IDs to distinguish them from one another. The presented vision tracking system is used to identify the positions and orientations of the three components by detecting the three fiducial markers. The whole process is a pick-move-and-place operation; the micro-gripper (ID 0) picks a micro-scale object (ID 16), and moves it (ID 16) near the reference (ID 1). These operations are monitored by the presented vision tracking system and the latest position information is sent to manipulation control software for proper operations. With this vision tracking system, the micro-manipulation can be implemented in an automatic method.

The micro-gripper (ID 0) consists of two thermally actuated gripping arms and is designed to pick up a target (ID 16) and release it. The picking up and relocation of the object is performed by a conventional 3 DOF micromanipulator. The location information of the target and the micro-gripper are monitored in real time and repre-
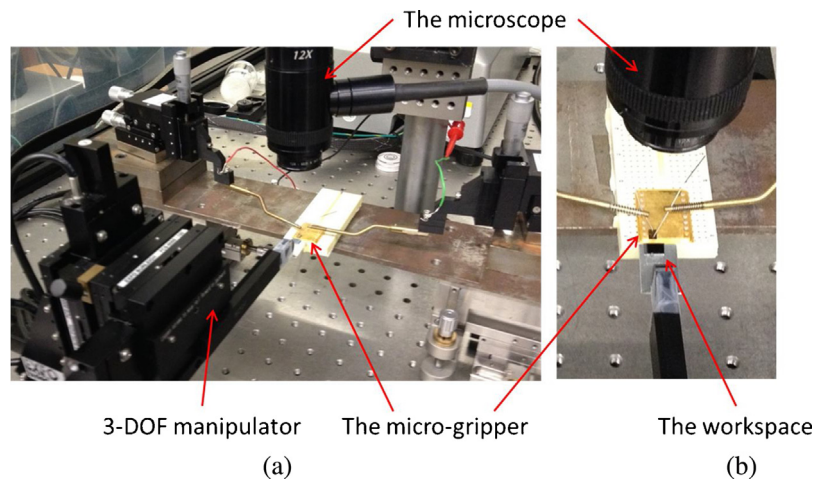
Fig. 11. Experimental set-ups for a micro-manipulation; (a) a full view, (b) a close-up view near the workspace.
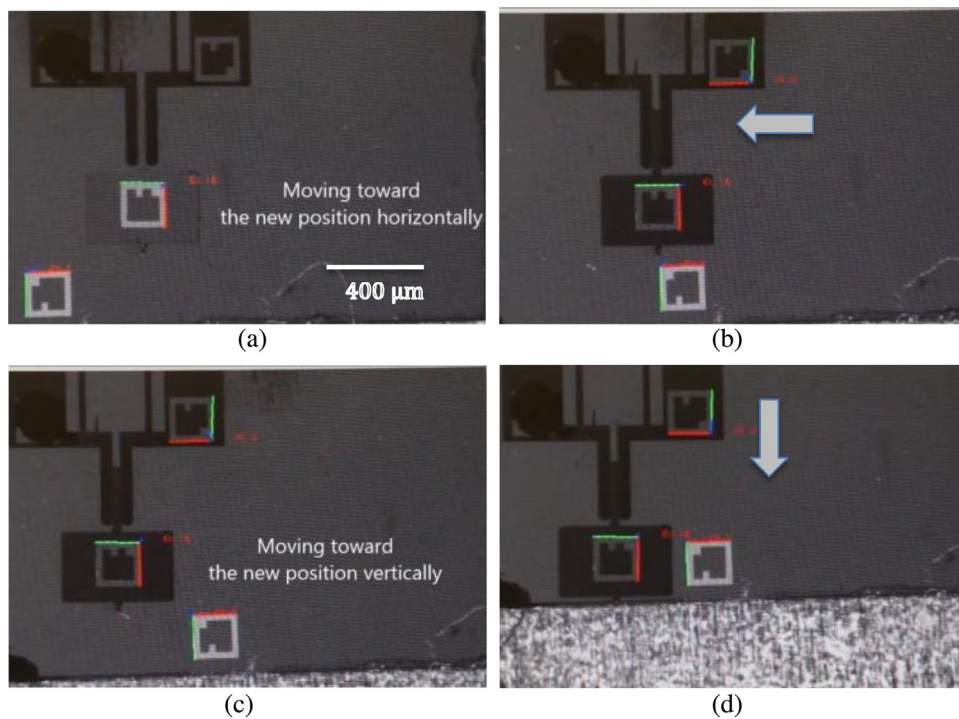

Fig. 12. Captured optical images of automated micro-manipulation operations; (a) the micro-gripper gripping a target, (b) the gripped target moving horizontally toward a target position, (c) the target stopped after the horizontal movement, and (d) the target moving down to a new position.

sented based on the position of the reference (ID 1) by the presented vision tracking system.

5.2. Demonstration of micro-manipulation

Based on the design of the micro-gripper and the vision-tracking system, the micro-manipulation system is set-up and shown in Fig. 11(a). The micro-gripper is fixed under the optical microscope and the workspace is installed on the conventional 3D manipulator. The target is placed on the workspace randomly within the field of view of the microscope, as shown in Fig. 11(b).

Some optical images captured during the micro-manipulation test are shown in Fig. 12. This manipulation is planned to pick a target on a workspace and move it to the left side of the reference.

At an initial stage, the vision tracking system starts scanning to find all fiducial markers within its field of view. All motions are monitored by the vision-tracking system in real time and the fiducial marker with ID 1 on the workspace is used as a reference. After obtaining the current position of the micro-gripper, the target, and a reference based on the detected ID information, the conventional 3D manipulator moves the workspace in a horizontal direction first and in a vertical direction later. The target is gripped by the two jaws of the micro-gripper as shown in Fig. 12(a). The vision tracking system detects the next position which is the lower left corner and recommends moving the target toward that direction. The movement is composed of horizontal first movement and vertical second movement. Next, the micro-gripper moves horizontally toward its subsequent position by measuring the relative distance between

the target and the reference on the workspace as seen in Fig. 12(b). When the vision tracking system determines that the horizontal distance is within an acceptable range, this horizontal movement stops as shown in Fig. 12(c). After this, the 3D manipulator starts moving vertically toward its future position right next to the reference fiducial marker in Fig. 12(d). This motion is stopped when the micro-gripper reaches its target position. The micro-gripper then will open its jaws to release the target object. With these operations, automated micro-manipulation based MEMS elements was demonstrated based on the presented vision tracking system and three fiducial markers.

6. Conclusion

The vision tracking system for MEMS devices or micro-scale objects was designed and tested to monitor the positions of micro-scale objects in real time. This presented system is composed of fiducial markers and corresponding detection algorithms. The predefined shape, called a fiducial marker, is utilized for fast motion tracking and good performance and implemented in MEMS with a metallization process. The accompanying detection algorithm is implemented based on an open computer vision library, OpenCV and geometric information of predetermined fiducial markers. From multiple experiments, the presented vision tracking system can recognize fiducial markers with an accuracy error less than 1%, a stability error less than 1 μm. Also, it is able to detect motions of a distance larger than 200 μm.

The presented vision tracking system is applied to a MEMS-based nanopositioner as a linear displacement sensor. With three fiducial markers, the presented system can calculate the self-calibrated displacement information. Another application to apply for is a micro-manipulation system as a position sensor. With presented system, multiple objects can be monitored in real time, so an automated micro-manipulation system is possible without serious design modification.

This vision tracking system has several advantages: (1) it requires no considerable design modification for MEMS devices, (2) it is cable-free and non-contact sensing, and (3) it is strong against any electric or thermal related noise. With these features, the presented system can be applied to various applications including micro-scale Augmented Reality (AR), 3D position measurement in MEMS devices, or multi-DOF sensing in MEMS motion stages.

Acknowledgements

References

[1] E. Eleftheriou, T. Antonakopoulos, G.K. Binnig, G. Cherubini, M. Despont, A. Dholakia, U. Durig, M. Lantz, H. Pozidis, H.E. Rothuizen, P. Vettiger, Millipede-a MEMS-based scanning-probe data-storage system, IEEE Trans. Magn. 39 (2003) 938–945.
[2] Y.-S. Kim, J.-M. Yoo, S.H. Yang, Y.M. Choi, N.G. Dagalaks, S.K. Gupta, Design, fabrication and testing of a serial kinematic MEMS XY stage for multifinger manipulation, J. Micromech. Microeng. 22 (2012).
[3] J. Wang, Z. Yang, G. Yan, Silicon-on-insulator out-of-plane electrostatic actuator with in situ capacitive position sensing, J. MicroNanolithogr. MEMS MOEMS 11 (2012) 1–33006.
[4] S. Avramov-Zamurovic, N.G. Dagalakis, R.D. Lee, Y.S. Kim, J.M. Yoo, S.H. Yang, Embedded capacitive displacement sensor for nanopositioning applications, Conference on Precision Electromagnetic Measurements (CPEM) (2010) 316–317.
[5] J. Wu, G.K. Fedder, L.R. Carley, A low-noise low-offset capacitive sensing amplifier for a 50 μg/$\sqrt{}$Hz monolithic CMOS MEMS accelerometer, IEEE J. Solid-State Circuits 39 (2004) 722–730.
[6] Y. Sun, B.J. Nelson, MEMS capacitive force sensors for cellular and flight biomechanics, Biomed. Mater. 2 (2007) S16.
[7] N. Yazdi, H. Kulah, K. Najafi, Precision readout circuits for capacitive microaccelerometers, Proceedings of IEEE Sensors 1 (2004) 28–31.
[8] J.T.M. Van Beek, P.G. Steeneken, B. Giesbers, A 10 MHz piezoresistive MEMS resonator with high Q, International Frequency Control Symposium and Exposition (IEEE) (2006) 475–480.
[9] A. Bazaei, M. Maroufi, A. Mohammadi, S.O.R. Moheimani, Displacement sensing with silicon flexures in MEMS nanopositioners, J. Microelectromech. Syst. 23 (2014) 502–504.
[10] T. Chen, L. Chen, L. Sun, J. Wang, X. Li, A Sidewall Piezoresistive Force Sensor Used in a MEMS Gripper, Intelligent Robotics and Applications, Springer, 2008, pp. 207–216.
[11] A. Bosseboeuf, S. Petitgrand, Application of Microscopic Interferometry Techniques In the MEMS Field Optical Metrology, International Society for Optics and Photonics, 2003, pp. 1–16.
[12] S. Bergna, J.J. Gorman, N.G. Dagalakis, Design and Modeling of Thermally Actuated MEMS nanopositioners ASME 2005 International Mechanical Engineering Congress and Exposition, American Society of Mechanical Engineers, 2005, pp. 561–568.
[13] A. Wang, H. Xiao, J. Wang, Z. Wang, W. Zhao, R.G. May, SElf-calibrated interferometric-intensity-based optical fiber sensors, J. Light. Technol. 19 (2001) 1495.
[14] O. Sasaki, H. Okazaki, M. Sakai, Sinusoidal phase modulating interferometer using the integrating-bucket method, Appl. Opt. 26 (1987) 1089–1093.
[15] O. Sasaki, K. Takahashi, Sinusoidal phase modulating interferometer using optical fibers for displacement measurement, Appl. Opt. 27 (1988) 4139–4142.
[16] O. Sasaki, T. Suzuki, Interferometric displacement sensors using sinusoidal phase-modulation and optical fibers vol 5633, (2005), 120–127.
[17] B.J. Vikramaditya, Visually guided microassembly using optical microscopes and active vision techniques, in Proceedings, IEEE International Conference on Robotics and Automation (1997) 3172–3177.
[18] M. Fiala, Comparing ARTag and ARToolkit Plus fiducial marker systems, IEEE International Workshop on Haptic Audio Visual Environments and their Applications (2005).
[19] M. Fiala, Vision guided control of multiple robots, First Canadian Conference on Computer and Robot Vision. Proceedings 2004 (2004) 241–246.
[20] Anon IEEE Xplore Abstract (Authors)—Indoor localization using laser scanner and vision marker for intelligent robot.
[21] G. Bradski, A. Kaehler, Learning OpenCV: Computer Vision with the OpenCV Library, O'Reilly Media, Inc., 2008.
[22] R. Laganière, OpenCV 2Computer Vision Application Programming Cookbook: Over 50 Recipes to Master this Library of Programming Functions for Real-time Computer Vision, Packt Publishing Ltd., 2011.
[23] N.M. Jokerst, M.A. Brooke, M.G. Allen, 1995 Processes for lift-off of thin film materials or devices for fabricating three dimensional integrated circuits, optical detectors, and micromechanical devices, US Patent US6214733 B1.
[24] Z. Zhang, Flexible camera calibration by viewing a plane from unknown orientations computer vision, 1999, The Proceedings of the Seventh IEEE International Conference on Vol. 1 (IEEE) (1999) 666–673.
[25] K. Miller, A. Cowen, G. Hames, B. Hardy, SOIMUMPs design handbook, MEMScAP Inc., Durh, 2004.
[26] Bosch DRIE process, US Patent 5501893.
[27] DMEMS Dynamic MEMS Measurement Option for Wyko NT1100 Optical Profilers, www2.veeco.com/pdfs.php/396

Biographies

Yong-Sik Kim received the Ph.D. degree at the University of Maryland, College Park. He received M.S. degree in mechanical engineering from the Korea Advanced Institute of Science and Technology (KAIST), Daejeon, Korea, in 2004. He is currently a Research Associate with the National Institute of Standards and Technology, Gaithersburg, MD. His research activity is mainly focused on the design, testing, and optimization of MEMS nanopositioners, MEMS microforce, and nanodisplacement sensors.

Seung Ho Yang received the M.Sc. and Ph.D. degrees in mechanical engineering from the Yonsei University, Seoul, Korea, in 1998 and 2002, respectively. From 1991 to 1998, he was with Samsung, Korea. From 1994 to 1996, he was involved in a joint research project between Samsung and the Russian Academy of Science. From 1996 to 2002, he was with the Korea Institute of Science and Technology (KIST). From 2003 to 2013 he was with National Institute of Standards and Technology (NIST). He is currently a staff engineer at SEAGATE Technology in Shakopee, MN. He has been a Reviewer of peer-reviewed journals, including Nanotechnology, Journal of Micromechanics and Microengineering, Measurement Science and Technology, Journal of Physics D, Philosophical Transactions of the Royal Society A, and Sensors and Actuators A. He is a coauthor of 28 scientific papers and 39 conference proceedings. He is a coholder of six patents. His research interests include nanomechanics, microelectromechanical systems, and tribology. Dr. Yang is an Affiliated Member of the American Society of Mechanical Engineers (ASME). He received the bronzemedal for Samsung's New Technology Award in 1996 and the KIST Academic Excellence Award in 2002. He received a Postdoctoral Fellowship from the Korean Government (Korean Science and Engineering Foundation) in 2002.

Kwang Woong Yang received the M.Sc. and B.Sc. degrees in automation engineering from Inha University, Inchon, Korea, in 1998 and 1996, respectively. From 1998 to 2002, he was with Dusan MechaTech. He is currently with Korea Institute of Industrial Technology. His research activity is mainly focused on Robot Software Architecture, Distributed Computing and Software Engineering.

Nicholas G. Dagalakis (SM'10) received the M.S., Eng.D., and Ph.D. degrees from the Massachusetts Institute of Technology (MIT), Cambridge, and theDiploma degree in mechanical and electrical engineering from the National Technical University of Greece, Athens, Greece. He has been with two small companies, with MIT as a Research Associate, and with the University of Maryland, College Park, as an Assistant Professor. In 1985, he joined the National Institute of Standards and Technology (NIST), Gaithersburg, MD, as a full-time Research Staff. He has conducted research in electrical generation, biomedical engineering, robotics, high-micromanufacturing/nanomanufacturing, sensors, and standards. Since 1999, he has been a Project Leader for several NIST- and other agency-funded projects. He is the author or a coauthor of 25 journal papers, 51 conference proceedings papers, four reports, and two books. He is the holder of two patents. Dr. Dagalakis is the recipient of the 2008 U.S. Senate Special Committee onAging Award and the 2009 NIST Bronze Medal Award.